Early developmental plasticity of lateral roots in response to asymmetric water availability

Daniel von Wangenheim[1,2], Jason Banda[1], Alexander Schmitz[2], Jens Boland[3], Anthony Bishopp[1], Alexis Maizel[3], Ernst H.K. Stelzer[2] and Malcolm Bennett[1]**

[1]Plant & Crop Sciences, School of Biosciences, University of Nottingham, LE12 5RD, UK.
[2]Buchmann Institute for Molecular Life Sciences, Goethe-Universität Frankfurt am Main, D-60438 Frankfurt am Main, Germany.
[3]Centre for Organismal Studies, Heidelberg University, D-69120 Heidelberg, Germany.

***Denotes co-corresponding authorship**

Abstract

Root branching is influenced by the soil environment and exhibits a high level of plasticity. We report that the radial positioning of emerging lateral roots is influenced by their hydrological environment during early developmental stages. New lateral root primordia have both a high degree of flexibility in terms of initiation and development angle towards the available water. Our observations reveal how the external hydrological environment regulates lateral root morphogenesis.

Main text

The soil environment contains a variety of niches for a growing root to explore. This complex environment consists of nutrient rich areas, air pockets, stones etc. and strongly varies in its moisture distribution, to which we refer as the hydrological landscape. The ability of a root system to absorb water and nutrients efficiently from a heterogeneous medium depends on its architecture and its ability to adapt to the available potential resources[1]. For example, plants generate lateral roots in nutrient rich patches and reduce branching in dry areas[2,3]. Similarly, roots emerge on that side of the primary root, which is in contact with moisture, a mechanism called hydropatterning[4,5]. Here we show that lateral root morphogenesis is steered by the available moisture during lateral root primordia initiation, while outgrowth stages and plasticity in organogenesis are likely directed by lateral root flanking cells.

Lateral roots originate primarily from the pericycle cell layer in both angiosperms and gymnosperms. The radial distribution of lateral roots is partly determined by the geometry of the root with respect to underlying phloem and xylem tissues[6]. *Arabidopsis* has a diarch root with two xylem poles and lateral roots initiate in the pericycle cells overlaying one xylem pole (Fig. 1A, B, Fig S1)[7,8]. In order to investigate how the vascular geometry of *Arabidopsis* affects the positioning of lateral root primordia in response to different moisture levels, we grow plants on an agar surface to expose roots to two distinct water environments, i.e. when one side is in contact with the agar (termed contact-side) versus humidity from the air (termed airside). We then captured 3D image stacks of roots grown on the agar surface using Light Sheet Fluorescence Microscopy (LSFM)(Fig. 1C, Fig. S2-S3, Supplemental Movie 1). We observed that both the orientation of the xylem pole axis and the lateral root primordium initiation site relative to the agar surface are uniformly distributed across the radius of the root. In the case of LRP initiation sites 54% orient towards the gel versus 46% towards the airside (Fig. 1D, E). This suggests that in our setup the choice of the initiation site is not influenced by a moisture gradient. However, 80% of the lateral root emergence angles are <90°, pointing towards the agar (Fig. 1C, D, E). When does this apparent asymmetry of the organ's emergence angle arise?

To investigate the angle of the lateral root outgrowth relative to the xylem pole, we define a line from the xylem pole to the tip of the primordium (Fig. 1C). The angle on top of the xylem pole is defined as 0°. Our experiments reveal that this angle varied by more than 70° (Fig. 1F, H). The primordia emerging on the airside orient mainly towards the gel surface. In contrast, primordia initiating on the contact-side orient mainly parallel to the gel surface. These results indicate that the lateral root outgrowth angle is highly plastic and steers organ development preferentially towards externally available water sources.

We tested whether external water availability is the stimulus for the orientation of the lateral root outgrowth when it grows along the agar surface. Hence, we quantified lateral root angles when grown embedded in gel or immersed in water to provide uniform mechanical or aqueous environments, respectively. In both cases we observed that the angles of the lateral roots' orientations were significantly smaller relative to the angles of roots grown on agar (Fig. 1G, H). Hence, when moisture is uniformly available, the lateral root outgrowth angles tend to distribute evenly and deviate less from the axis of xylem poles.

Next, we investigated at which developmental stage(s) the bias in lateral root emergence angle arises. Lateral root primordia originate from dividing cells located in 5-8 adjacent pericycle cell files, which undergo a series of anticlinal, periclinal and then radial divisions[9–12]. Earlier studies have reported the importance of the cell file directly overlying the xylem pole during lateral root morphogenesis in *Arabidopsis*[8,10,13]. This "central" cell file forms the tip of the primordium and contributes most of the cell mass at the time of emergence[12]. However, the role of flanking cell files could be more important than previously reported. To uncover the contribution of each cell file, we manually tracked cell contours in a transversal cross section post emergence in two independent experiments (Fig. 2A). This analysis revealed that all cell files contribute to the final lateral root primordium, but flanking cell files continue to contribute to a primordium's volume, whereas the central cell file provides only a thin cell file (Fig. 2A). This highlights that all contributing pericycle cell files play an important role through different stages of lateral root morphogenesis.

The contribution of individual cell files is highly variable[12]. This could be due to differences in radial division rates between cell files, which increases the width of the primordium (Fig. 2B). To address this possibility, we re-analyzed five published datasets[12] and observed that the occurrence of radial divisions varied (Fig. 2C). In datasets #121211 and #130607 radial divisions occurred preferentially on one side of the primordium, resulting in an asymmetric increase in width (Fig. 2C). Hence, although these images were acquired submerged in a light sheet microscope's specimen chamber, they reveal plasticity in the direction of radial growth. Even in these datasets, radial divisions promote growth along a particular direction and provide a basis for influencing the angle of the lateral root outgrowth.

The direction of lateral root outgrowth is determined by the radial cell divisions in flanking files. However, there are earlier events that influence the angle of outgrowth. Recently we reported the expression of the early lateral root marker *pLBD16::LBD16:GFP*[14] preferentially in pericycle cells facing the agar (contact-side)[5]. To investigate the radial position of early events during lateral root initiation relative to the xylem pole axis, we captured the expression of LBD16:GFP with respect to the xylem pole. In 39 lateral root primordia datasets we observed 13 cases, in which LBD16 expression was not strictly above the xylem pole (Supplemental Figure 4). In Figure 2D-F (and Supplemental Movie 2) we show the most extreme examples of deviations in central cell file location relative to the xylem pole axis. The migration of nuclei prior to the first cell division (Fig. 2D), the first anticlinal cell division (Fig. 2E) and the first periclinal division (Fig. 2F) were observed in different plants independently. Hence, the selection of pericycle cell files that contribute to a new lateral root primordium takes place at a very early developmental stage, i.e. prior to the first cell division. We showed previously that developmental plasticity drives the selection of cells along the longitudinal axis of the root[12]. Our new findings reveal that developmental plasticity also exists in the radial axis.

We conclude that external water availability profoundly influences lateral root formation during organ emergence. Lateral roots are critical for exploring large volumes of soil for nutrients and moisture. To acquire water efficiently, plants have developed mechanisms that drive lateral root outgrowth towards

external water availability[4,5]. In contrast to these earlier studies, which focused on the underlying molecular mechanisms that control this behavior, this study focused on cell to organ scale mechanisms that contribute to the outgrowth of the LRP in response to water availability. Our study reveals that, unlike the xylem pole axis, the selection of pericycle cell files that initiate a new lateral root primordium is linked to the external hydrological landscape. Our results also reveal that radial divisions steer outgrowth of the LRP. These two mechanisms potentially steer LRs towards external water. The strong impact of the hydrological landscape explains the non-stereotypical patterns of division reported for the morphogenesis of lateral root primordia[11,12]. Collectively, our observations suggest that the external hydrological environment regulates lateral root organogenesis from initiation to outgrowth, and represents a potential adaptive advantage when foraging under heterogeneous soil conditions.

Materials and Methods

Plant material and growth conditions

Arabidopsis thaliana ecotype, Columbia (Col-0) was used as wild type. The reporter line pLBD16::LBD16-GFP was previously published[14]. *Arabidopsis thaliana* seed lines were surface sterilized using 10 % (v/v) bleach for 3 min containing 0.001 % Triton X-100 followed by five washes with sterile water and then stratified at 4 °C for 48 h in the dark. Seeds were germinated on media containing ½ MS (2.15 g/L) (Murashige and Skoog media, Sigma), 0.97 g/L MES, 1 % sucrose and 1 % Bacto agar at pH 5.7. Seedlings were grown vertically for 10 days under continuous temperature 22 °C with a 16 h photoperiod (150 µmol m−2 s−1). The same medium plates were used to let plants grow in the gel. Plants in the hydroponic experiments were grown 96-well plates with roots immersed in Hoagland's medium.

Light Sheet Fluorescence Microscopy[15] using the Zeiss Lightsheet Z.1 for outgrowth angle measurements

Arabidopsis thaliana seedlings were carefully (without moving them) glued on the media plate using 1% agarose. Root segments (3cm in length from the root tip) were cut out including the gel and transferred to a sample holder described earlier (Figure S1)[16]. The entire volume of the root was captured including the gel substrate using a 405 nm laser (laser intensity in ZEN set to 35%). Auto-fluorescence was filtered between 505-545 nm. The angles of the xylem pole axis and of the lateral root relative to the surface of the medium were measured in a cross section using ImageJ/Fiji (ImageJ version 1.52n)[17]. The line tool was used to draw a line parallel to the surface of the gel. Angles of xylem were measured by drawing a line from one xylem pole (the xylem without the primordium) to the other xylem pole (the xylem adjacent to the primordium). The angle of the lateral root primordium was measured by drawing a line from the xylem (adjacent to the primordium) to the tip of the primordium. Angles were exported from Fiji and normalized to the angle of the surface of gel. Since the angles measured in Fiji cover the range between -180° and +180°, the angles used in this paper were 1) transformed to become all positive between 0° and 360° and 2) rotated for the angle 0° to be perpendicular to the gel surface and 180° pointing into the air. The angles of the lateral roots are presented as follows: a) orientations towards the gel have positive values and b) those away from the gel have negative values. When xylem angles are smaller than 180° (on the right side of the radius) the angle becomes the difference "xylem angle minus lateral root angle" otherwise "lateral root angle minus xylem angle".

Data visualization:

Angle measurements were visualized using Adobe After Effects (version 16.1.2) (Figure 1d, g; Supplemental Figure 3; and Supplemental Movie 1). Three dimensional data visualization was performed using the software Arivis Vision 4D (version 3.1.2.) (Figure 1a, b; Figure 2 c, d-g; Supplemental Figure 4 and Supplemental Movie 2). Figures were assembled in Adobe Photoshop (version 20.0.5) and Adobe Illustrator (version 23.0.3)

Multi-view Light Sheet Fluorescence Microscopy (Figure 1A, B):

Arabidopsis thaliana seedlings were grown on the surface of media plates (½ MS + 1.0% bacto agar). Roots were covered with 1% agarose containing fluorescent beads (PS-Speck, fluorescent beads, ThermoFisher, Catalog number: P7220) and further processed according to the protocol depicted in Supplemental Fig. S2. Roots were imaged with a Zeiss Lightsheet Z1 microscope. Images were captured using the W Plan-Apochromat 20x/1.0 and the PCO.edge camera module (CMOS, 1920x1920 pixel). Excitation wavelengths: 405 nm for autofluorescence for YFP. Emission filter: Bandpass 505-545 nm for GFP and Bandpass 525-545 nm for YFP. Multi-view images were set up using the Quick-Setup option in the ZEN software. Single views were fused using the bead-based registration using the Fiji plugin Multiview Reconstruction[18,19]

Data availability statement:
Fig 1 F data freely available on the following link: https://youtu.be/A3qsY1evmQ0. Other data sets can be shared when requested.

Statistical methods:
All statistics were run in IBM SPSS statistics 24. All assumptions for one-way ANOVA were tested and met (verified using distribution plots and Levene's test). Different letters indicate significant difference between treatments ($p<0.05$).

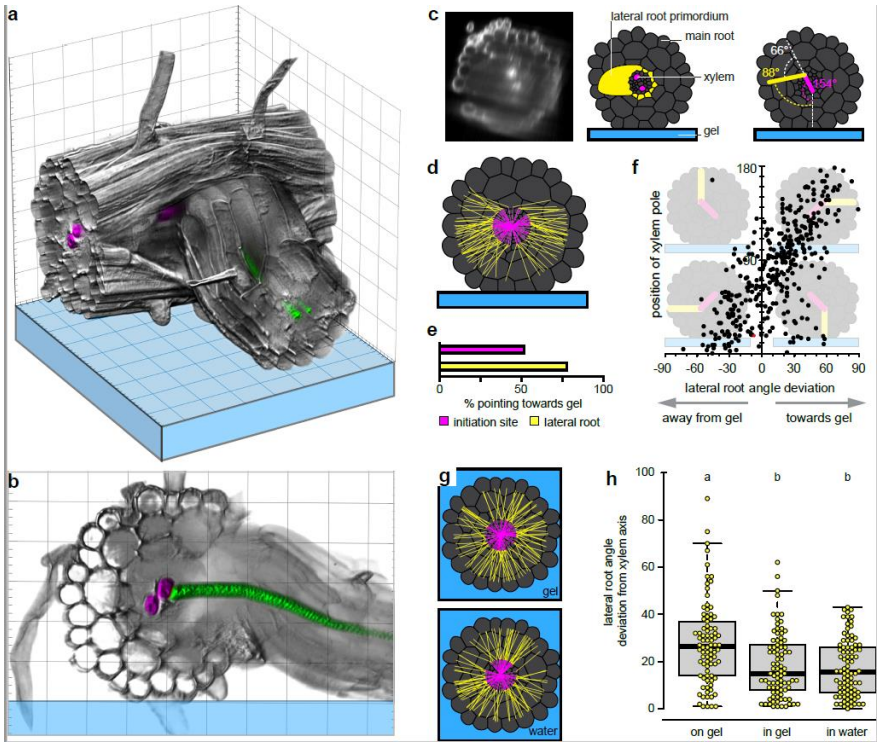

Figure 1: Arabidopsis branching is influenced by the root's position in the agar. a) A three-dimensional (3D) rendering of the auto-fluorescence signal of a lateral root grown out of the main root captured by multi-view light sheet fluorescence microscopy. b) The two xylem strands of the lateral root (green) are connected to one of the two xylem strands of the main root (magenta). Scaling boxes are 25 µm in size, tick marks 5 µm. c) Autofluorescence 3D light sheet imaging of a young primordium (left), a schematic (middle) and the corresponding angles (right) of the xylem axis (magenta) and the lateral root (yellow) relative to the gel surface. The white angle represents the orientation of the lateral root relative to the xylem axis. d) The complete overlaid set of n=87 angle measurements based on n=10 biological independent samples, data set #180912). e) Percentage of lateral roots oriented towards the gel, i.e. <90° with respect to the agar surface (data set #180912, n=87). f) Lateral root angle deviation relative to the xylem axis plotted against the position of xylem relative to the gel surface. Lateral roots orient towards the agar when initiation occurs on the airside (upper right) and away from the gel when initiation faces the contact side (lower left). No lateral root is oriented towards the air when initiation occurs on the airside (upper left). The data is derived from five independent experiments. In total, 352 primordia from 42 plants were analyzed (see Supplemental Figure 3). Bivariate Pearson Correlation was used to test the linear relationship between the position of the xylem pole and the lateral root outgrowth angle. A strong positive correlation was found with $r = 0.726$ ($p=7.8545E-59$; 2-tailed test) g, h) Lateral roots grown in gel or water have a smaller deviation angle relative to the xylem pole axis than those grown on gel. Data derives from one experiment, 87 images were analyzed per condition. Centerlines show the medians. Box limits

indicate the 25th and 75th percentiles as determined by R software (https://www.r-project.org/); whiskers extend 1.5 times the interquartile range from the 25th and 75th percentiles, data points are plotted as yellow circles. Statistical differences were analyzed using one-way analysis of variance (ANOVA), Tukey HSD test (P<0.0001; 95% Confidence Interval). Statistically similar groups use the same letters.

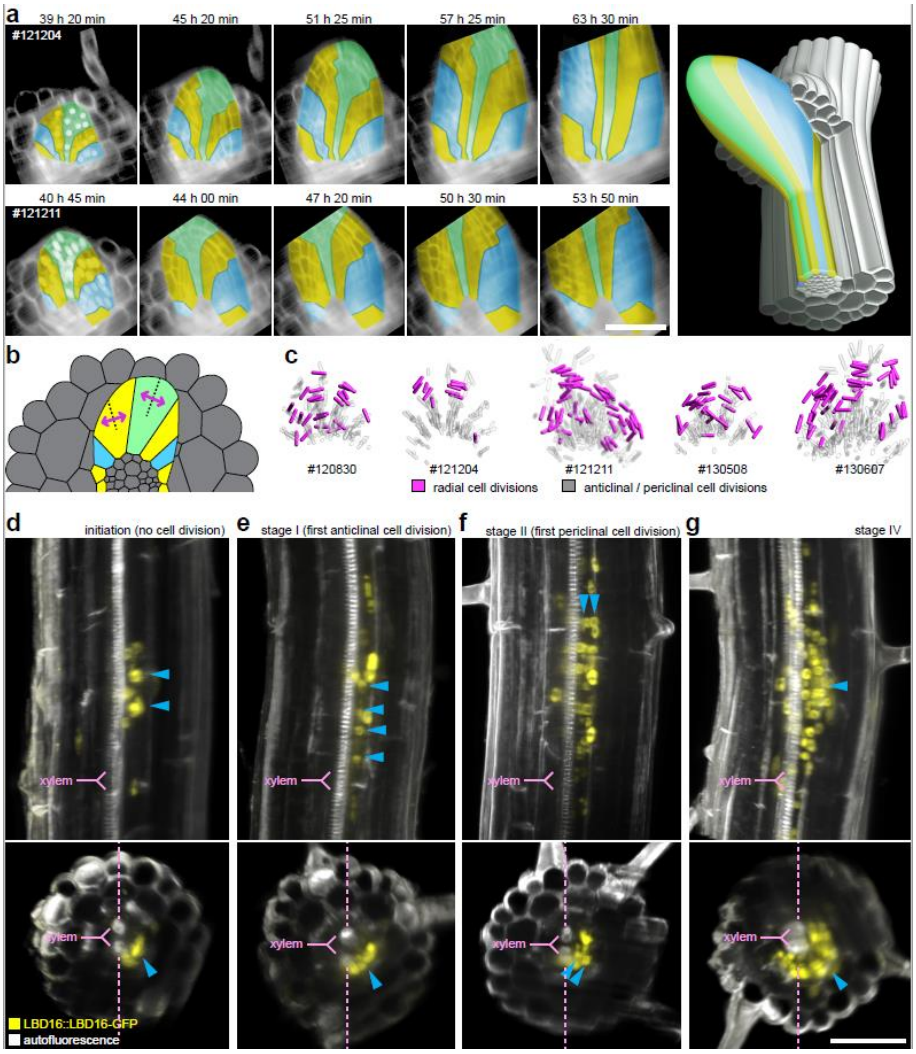

Figure 2: Lateral root development is flexible during all developmental stages. a) Cell files tracking from 3D light sheet fluorescence microscopy time course data sets[12] of two biological independent experiments. The colour of the cell file indicates which group of cells derive from the same mother cell. Here the green cells represent the central cell file. They derive from the cell that undergoes the first periclinal division on its way to become a lateral root primordium. This figure illustrates that the contribution of flanking cell files (yellow and blue cell files) increases over time and pushes the central cell file out of the main root. b) Schematic of radial divisions in some cell files, which increases the width of the primordium. c) Cell division pattern analyses from five biological independent time course data reveal that radial divisions occur preferentially on one side. Thus, the lateral root bends along one direction. d-g) Four individual roots show the expression pattern of LBD16 during the first stages of lateral root development, i.e. the migration of nuclei before the first cell division (d), the first anticlinal cell division (e), the first periclinal division (f) and a stage IV primordium (g). The central file is not strictly above the xylem pole. 39 primordia were scanned, in three independent experiments in which 14 times the central file was not in line with the xylem pole axis (Supplemental Figure 4). Scale bar: 50 µm.

References

1. Morris, E. C. *et al. Curr. Biol.* **27,** (2017).
2. Drew, M. C. *New Phytol.* **75,** 479–490 (1975).
3. Orman-Ligeza, B. *et al. SSRN Electron. J.* (2018). doi:10.2139/ssrn.3188447
4. Bao, Y. *et al. Proc. Natl. Acad. Sci. U. S. A.* **111,** 9319–24 (2014).
5. Orosa-Puente, B. *et al. Science (80-.).* **362,** 1407–1410 (2018).
6. Guttenberg, H. v. in *Handbuch der Pflanzenanatomie* (ed. Linsbauer, K.) Band 8 (Gebrüder Bornträger, 1940).
7. Casero, P. J., Casimiro, I. & Lloret, P. G. *Protoplasma* **188,** 49–58 (1995).
8. Laskowski, M. J., Williams, M. E., Nusbaum, H. C. & Sussex, I. M. *Development* **121,** 3303–3310 (1995).
9. Casimiro, I. *et al. Plant Cell* **13,** 843–852 (2001).
10. Dubrovsky, J. G., Rost, T. L., Colón-Carmona, A. & Doerner, P. *Planta* **214,** 30–36 (2001).
11. Lucas, M. *et al. Proc. Natl. Acad. Sci. U. S. A.* **110,** 5229–5234 (2013).
12. von Wangenheim, D. *et al. Curr. Biol.* **26,** (2016).
13. Casimiro, I. *et al. Trends Plant Sci.* **8,** 165–171 (2003).
14. Goh, T., Joi, S., Mimura, T. & Fukaki, H. *Development* **139,** 883–893 (2012).
15. Stelzer, E. H. K. *Nat. Methods* **12,** 23–6 (2015).
16. von Wangenheim, D., Hauschild, R. & Friml, J. *J. Vis. Exp.* **2017,** (2017).
17. Schindelin, J. *et al. Nat. Methods* **9,** 676–682 (2012).
18. Preibisch, S., Saalfeld, S., Schindelin, J. & Tomancak, P. *Nat. Methods* **7,** 418–419 (2010).
19. Preibisch, S. *et al. Nat. Methods* **11,** 645–648 (2014).

Correspondence and requests for materials should be addressed to M.B.

Acknowledgments
This work was supported by the awards from the Biotechnology and Biological Sciences Research Council [grant numbers BB/M012212, BB/G023972/1, BB/R013748/1, BB/L026848/1, BB/M018431/1, BB/PO16855/1, BB/M001806/1]; European Research Council FUTUREROOTS Advanced Investigator grant 294729; and Leverhulme Trust grant RPG-2016-409. Ernst Stelzer is funded by the Deutsche Forschungsgemeinschaft (CEF-MC I/II, DFG Exc 115). Work of the Maizel lab is supported by the DFG FOR2581, the Land Baden-Württemberg, the Chica und Heinz Schaller Stiftung, the CellNetworks cluster of excellence and the Boehringer Ingelheim Foundation.

Author contributions: D.W., J.B., A.B., A.M., E.H.K.S., and M.B. designed experiments; D.W. and J.B. performed experiments; D.W., J.B., A.S., J.B., A.B., A.M., E.H.K.S., and M.B. analysed the data; and D.W., J.B. and M.B. wrote the manuscript with contributions from all other aut

Competing interests
The authors declare no competing interests.